Geomechanics and Engineering, *Vol. 7*, *No. 6* (*2014*) *589-612*
DOI: http://dx.doi.org/10.12989/gae.2014.7.6.589

Assessment of liquefaction potential of the Erzincan, Eastern Turkey

Esra Subaşı Duman [1a], Sabriye Banu Ikizler [*2], Zekai Angın [2b] and Gökhan Demir [3c]

[1] *Civil Engineering Department, Turgut Ozal University, Ankara, 06010, Turkey*
[2] *Civil Engineering Department, Karadeniz Technical University, Trabzon, 61080, Turkey*
[3] *Civil Engineering Department, 19 Mayıs University, Samsun, 55139, Turkey*

(*Received January 30, 2014, Revised August 07, 2014, Accepted August 11, 2014*)

Abstract. This study includes determination of liquefaction potential in Erzincan city center. Erzincan Province is situated within first-degree earthquake zone on earthquake map of Turkey. In this context, the earthquake scenarios were produced using the empirical expressions. Liquefaction potential for different earthquake magnitudes (6.0, 6.5, 7.0) were determined. Liquefaction potential was investigated using Standard Penetration Test (SPT). Liquefaction potential analyses are determined in two steps: geotechnical investigations and calculations. In the first steps, boreholes were drilled to obtain disturbed and undisturbed soil samples and SPT values were obtained. Laboratory tests were made to identify geotechnical properties of soil samples. In the second step, liquefaction potential analyses were examined using two methods, namely Seed and Idriss (1971), Iwasaki *et al*. (1981). The liquefaction potential broadly classified into three categories, namely non-liquefiable, marginally liquefiable and liquefiable regions. Additionally, the liquefaction potential index classified into four categories, namely non-liquefiable, low, high and very high liquefiable regions. In order to liquefaction analysis complete within a short time, MATLAB program were prepared. Following the analyses, liquefaction potential index is investigated by Iwasaki *et al*. (1982) methods. At the final stage of this study, liquefaction potential maps and liquefaction potential index maps of the all study area by using IDW (inverse distance weighted) interpolation method in Geostatistical Analyst Module of ArcGIS 10.0 Software were prepared for different earthquake magnitudes and different depths. The results of soil liquefaction potential were evaluated in ArcGIS to map the distributions of drillings with liquefaction potential. The maps showed that there is a spatial variability in the results obtained which made it difficult to clearly separate between regional areas of high or low potential to liquefy. However, this study indicates that the presence of ground water and sandy-silty soils increases the liquefaction potential with the seismic features of the region.

Keywords: liquefaction; liquefaction potential; liquefaction potential index; earthquake; geostatistical analysis; standard penetration test

1. Introduction

Located in one of the world's most seismically active continental regions, Turkey has a long

*Corresponding author, Assistant Professor, E-mail: banuh73@gmail.com
[a] Ph.D. Student, E-mail: subasi_esra_53@hotmail.com
[b] Assistant Professor (or Ph.D.), E-mail: angin@ktu.edu.tr
[c] Assistant Professor (or Ph.D.), E-mail: gokhandemir61@gmail.com

http://www.techno-press.org/?journal=gae&subpage=7 ISSN: 2005-307X (Print), 2092-6219 (Online)

history of frequent and destructive earthquakes. The more stable part of central Turkey has relatively few earthquakes, whereas the East Anatolian Fault Zone has moderate seismicity. The North Anatolian Fault Zone (NAFZ) has been the source of many damaging earthquakes during the twentieth century: the most of earthquakes ranging in magnitude from 6.5 to 7.9 have occurred in this zone (Gurenko *et al*. 2006). Erzincan Province is an old town situated in the North Anatolian fault zone and North Anatolian Fault Zone is located approximately 7.7 km from Erzincan city center. Erzincan Basin has been affected by large earthquakes associated with the North and East Anatolian fault zones. Erzincan Basin, where soil conditions are highly heterogeneous, is composed of alluvial deposits of sand and gravel with very small amounts of clay and silt (Saatcioglu and Bruneau 1993). There is liquefaction potential in Erzincan due to the Euphrates River near the city, earthquake hazard and soil conditions. Therefore, assessment of liquefaction potential Erzincan is an important study.

Many methods have been suggested to develop liquefaction potential models by researchers, which based on field testing data, such as Standard Penetration Test (Seed and Idriss 1971, Tokimatsu and Yoshimi 1983, Iwasaki *et al*. 1981), cone penetration test (Seed and De Alba 1986, Suzuki *et al*. 1997, Robertson and Wride 1998). The standard penetration test (SPT) data are very common in deciding the liquefaction potential in geotechnical engineering. The standard penetration test (SPT) to determine factor of safety (F_S) were used at the many studies (Yalcin *et al*. 2008, Tosun *et al*. 2011, Orhan *et al*. 2013, Zhang *et al*. 2013). In the literature, assessments of liquefaction potential are available for different regions and structures using this method (Ansal and Tönük 2007, Mhaske and Choudhury 2010, Samui and Sitharam 2011, Choobasti *et al*. 2012a and b). Many provinces of Turkey such as Eskişehir, Aksaray, Sakarya and Hatay, liquefaction potentials were determined using SPT values. In addition, laboratory studies were done to determine liquefaction potential of soils (Shooshpasha and Bagheri 2014, Sandoval and Pando 2012, Krim *et al*. 2013, Choobbasti *et al*. 2013).

SPT-based simplified empirical procedure is widely used for assessment liquefaction potential of soils. Factors of safety (F_S) along the depth of soil profile are an important parameter. The factor of safety values are classified three categories, namely, liquefiable ($F_S \leq 1.0$), marginally liquefiable ($1.0 < F_S \leq 1.2$) and, non-liquefiable ($1.2 < F_S$). Although F_S shows the liquefaction potential of a soil layer at a particular depth in the subsurface, it does not show the degree of liquefaction potential at liquefiable areas. Liquefaction potential index was developed to estimate the potential of liquefaction to cause foundation damage at an area. Iwasaki *et al*. (1982) proposed classification categories called as non-liquefiable ($I_p = 0$), low ($0 < I_p \leq 5$), high ($5 < I_p \leq 15$), and very high ($15 < I_p$) for liquefaction potential. Dixit *et al*. (2012) investigated liquefaction potential index at Mumbai city based on the method proposed by Iwasaki *et al*. (1982). Sonmez and Gokceoglu (2005) proposed classification categories called as non-liquefiable ($I_p = 0$), low ($0 < I_p \leq 2$), moderate ($2 < I_p \leq 5$), high ($5 < I_p \leq 15$) and very high ($15 < I_p$) for liquefaction potential. The liquefaction potential of the Aksaray province was investigated using Sonmez and Gokceoglu (2005) method (Yalçın *et al*. 2008).

In this paper, calculations were performed using Seed and Idrıss (1971), Iwasaki *et al*. (1981) and (1982) methods in order to determine liquefaction potential and index of Erzincan city center. SPT values were obtained and laboratory tests were made to identify physical properties of soil samples. Liquefaction potential and index for different earthquake magnitudes (6.0, 6.5, 7.0) were determined. The liquefaction maps were prepared by considering the liquefaction severity categories for different depths and different earthquake magnitudes using ArcGIS 10.0 Software. The analyses and maps showed that there is diversity in the study area in terms of liquefaction potential.

2. Geology of the study area

Erzincan Basin is situated in eastern Turkey, at 39°32’-39°52’ latitude and 39°15’-39°50’ longitude. The province of Erzincan is a highly mountainous region with an area of 11,900 km². The city sits in a basin measuring 50 km east-west by 15 km north- south, at an altitude of 1200 above sea level, surrounded on all sides by mountains rising to heights in excess of 3000 m. The whole plain 45-50 km long and 4-20 km wide in northwest-southeast direction is located within the boundaries of Erzincan. The elevation of plain from sea level is 1140 m. Erzincan Plain is surrounded by 3500 m high Mount Kesis in the north, more than 3500 m high Mount Munzur in the south and Karadag in the west. Karasu which is a river reach of Euphrates and other influent streams create large planes on Erzincan plain. There is a big fault system in the north of Erzincan plain.

The principal geological feature of the affected area is Erzincan Basin (Fig. 1). Formation of the basin was initiated by pull-apart motion between two divergent segments of the North Anatolian Fault; subsequently development is complex and incompletely understood. The center of the basin is filled with alluvial plain deposits, consisting of silts, sands and gravels. These comprise rather more loose material than the alluvial fan deposits which predominate around the edges of the basin.

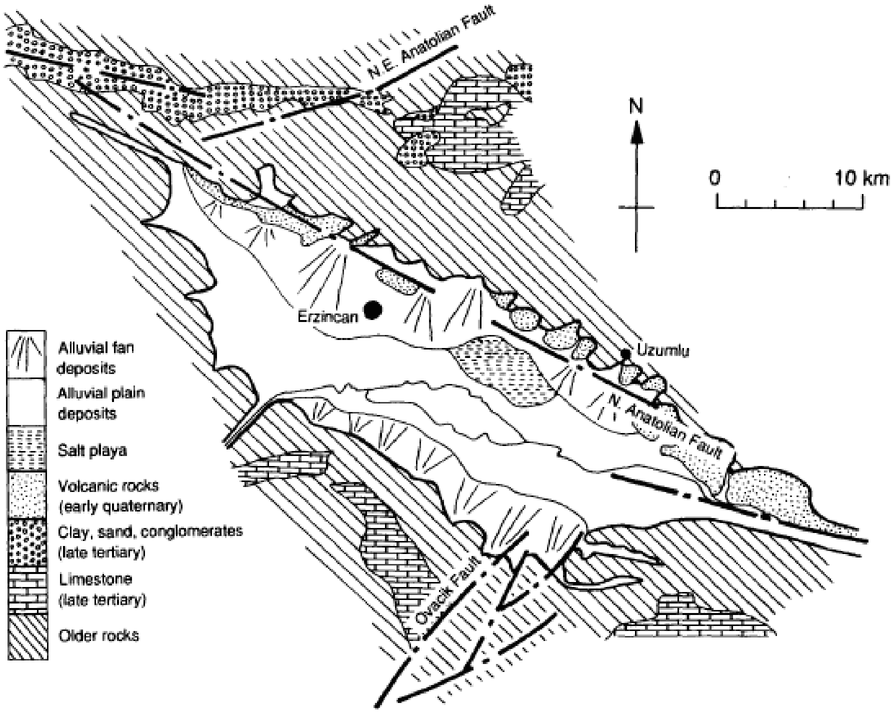

Fig. 1 Simplified geological plan of the Erzincan Basin

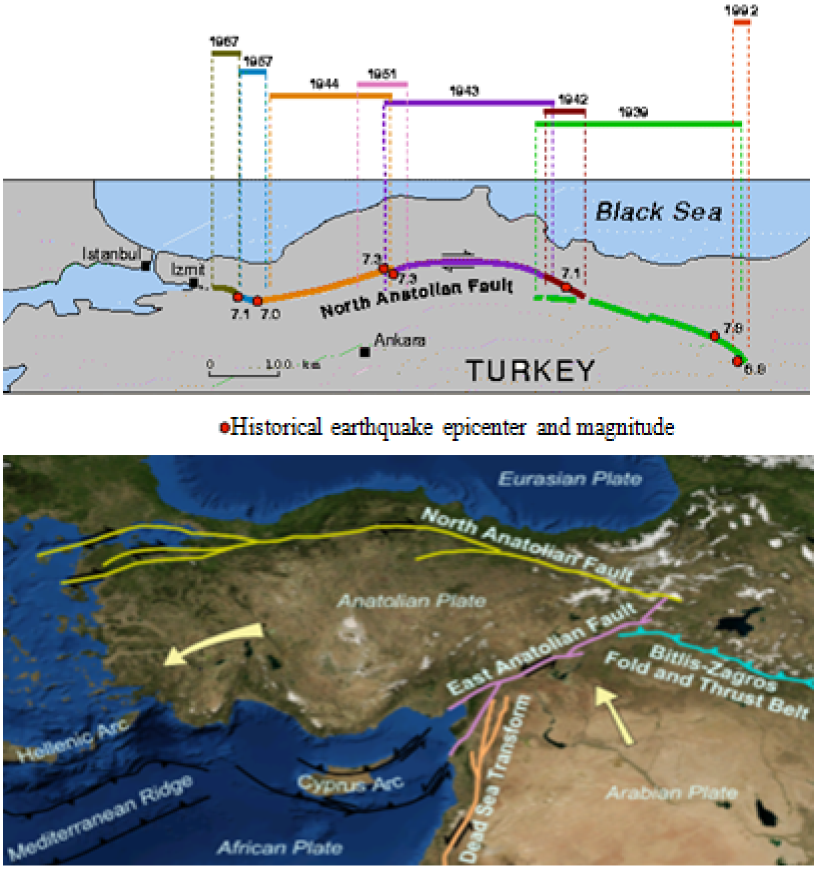

Fig. 2 Turkey seismic hazard zones and historical earthquakes in NAFZ

3. Seismotectonics of the study area

The Erzincan basin and vicinity in the North Anatolian Fault zone, which is the most active and the longest fault system of Turkey (Fig. 2), display a fairly complex structure in terms of its geologic, tectonic, and morphologic features. This region where many earthquakes with varying magnitudes occurred during the historical period is seismologically very active (Kaypak 2002).

Erzincan basin and its vicinity located on North Anatolian Fault Zone (NAFZ). The area where numerous earthquakes (Table 1) in various magnitudes have taken place during historical era is very active in seismologic sense (Kaypak 2002). In the last century two destructive earthquakes have occurred causing significant loss of life in the province of Erzincan. The 1939 (M=7.9) earthquake which is the first and the largest event (Emre *et al*. 2010). As a result of this earthquake; nearly 360 km long surface rupture occurred from Erzincan to Erbaa, then towards Amasya. 1939 earthquake started with a large compressing flexure towards the east end of surface rupture and the rupture moved mostly towards west. Surface faulting between Erzincan-Niksar basins followed the main route of North Anatolia Faulting Zone (NAFZ). However, in the most west section which is 76 km. long; surface faulting diverged from the main route and turned towards Ezinepazarı (Amasya) faulting route (Emre *et al*. 2010). Following this earthquake which

Table 1 Some historical earthquakes in Erzincan

Date	Magnitude (M)	Date	Magnitude (M)
1907	4.9	1960	5.9
1929	5	1961	4.5
1930	5.6	1964	4.9
1935	5	1965	5.6
1937	4.7	1966	4.6
1939	7.9	1967	5.9
1940	5.2	1968	4.5
1941	5.9	1969	4.7
1949	5.3	1970	5.3
1950	4.9	1979	4.6
1954	4.6	1980	4.6
1957	5.1	1983	5
1958	5.1	1992	6.8

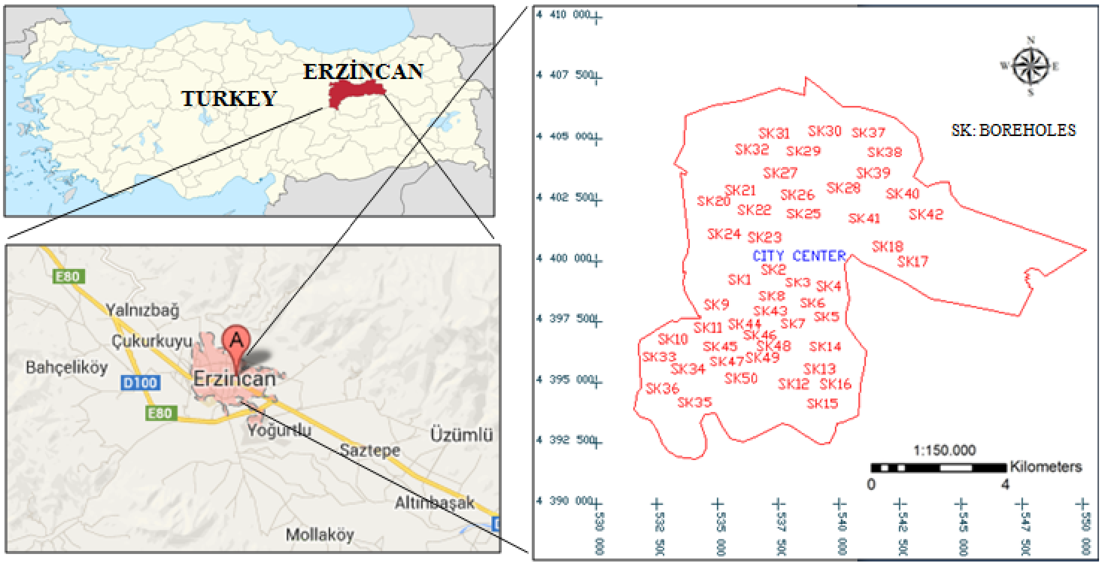

Fig. 3 Test holes at different locations

triggered earthquakes during 1939-1967 on NAFZ, seismic activity shifted towards west, and the following earthquakes took place in the east and west ends of faulting system.

Another important earthquake that took place on Erzincan Basin was the one in 1992 with the magnitude of 6.8. The 1992 Erzincan, Turkey, earthquake is the largest earthquake that occurred near Erzincan since the devastating earthquake (M=8) in 1939. This earthquake was the second most devastating earthquake after 1939 great disaster due to its way of formation, seismic features and the damage it caused. Erzincan earthquake which took place in 1992 is between the east end of

360 km section of North Anatolia Fault which was torn in 1939 earthquake and the east of Erzincan.

4. Field and laboratory properties of the study area

In this study, Erzincan city center was chosen as the study area. Areas which are contained in the study area are as follows: State building (1), Private Hospital, Hospital (1), Hospital (2), State building (2), Home for the aged, treatment plant, State building (3), and Industry area. Site conditions play a major role in the liquefaction of soil during seismic events. The SPT-Nvaluesare important for the liquefaction potential analysis. In the field stage, 50 boreholes in different locations were drilled to obtain N values. Test holes at different locations are shown in Fig. 3. The depths of measured values N changed between 1.5 and 24.0 m. Different soil types were observed in the study area.

The lowest SPT blow counts are observed in regions where ground water level near the surface of the ground, whereas at deeper levels, high SPT values are obtained. Average of SPT values is changed between 20 and 30. Test holes at different locations were obtained to determine index

Table 2 Field properties of the soil samples

Investigation area	Depth (m)	Boreholes	N value					Ground water level (m)
			Sample amount	Min.	Max.	Mean	Std. Deviation	
State Building (1)	4-20	SK1-SK5	60	22	36	29.5	2.77	12
Private Hospital	3-18	SK6-SK10	60	22	36	29.5	2.77	15
Hospital (1)	3-7.5	SK11-SK18	56	35	57	48.2	4.12	20
Hospital (2)	3-20	SK19-SK26	88	21	40	28.5	3.99	18
State Building (2)	3-9	SK27-SK29	29	14	47	31	10.1	19
Home for the aged	3-20	SK30-SK32	30	26	50	40.6	7.89	9.5
Treatment Plant	3-10.5	SK33-SK36	24	19	30	23.6	3.04	1
State Building (3)	3-18	SK37-SK42	88	21	40	28.5	3.99	20
Industry area	3-18	SK43-SK50	88	21	40	28.5	3.99	9.5

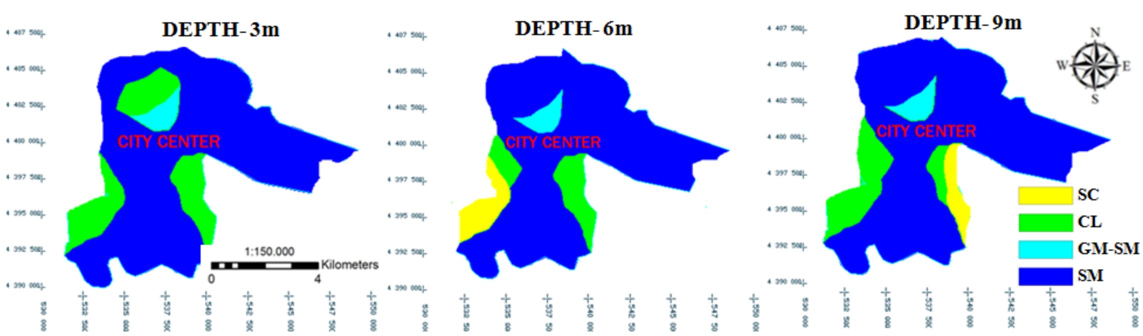

Fig. 4 Soil class zonation maps

properties of soils disturbed and undisturbed soil samples. Ground water levels were determined. Ground water levels changed between 1 and 20 in the study area. The field properties of the soil samples are shown in Table 2. The physical properties of the soil samples were tested in laboratory. Disturbed and undisturbed soil samples were determined physical properties such as grain size distribution, Atterberg limits, unit weight, water content and type of soil. According to USCS (Unified Soil Classification System), in the study area soils can be classified as SM (silty sand), GM (silty gravel), CL (inorganic clay). The major part of the study area was classified as SM. Soil class zonation maps of the study area are shown in Fig. 4.

In this study area, the values of unit weight changed between 18.1 kN/m^3 and 20.15 kN/m^3 and average is 18.7 kN/m^3. The values of water content changed between 4.1% and 27% and average is 16.62%. The Atterberg limits in the study area are quite variable. In most places, soil was determined as none-plastic. Position of the samples on a plasticity chart is shown in Fig. 5.

The values of liquid limit changed between 24% and 52% and average is 38.96%. The values

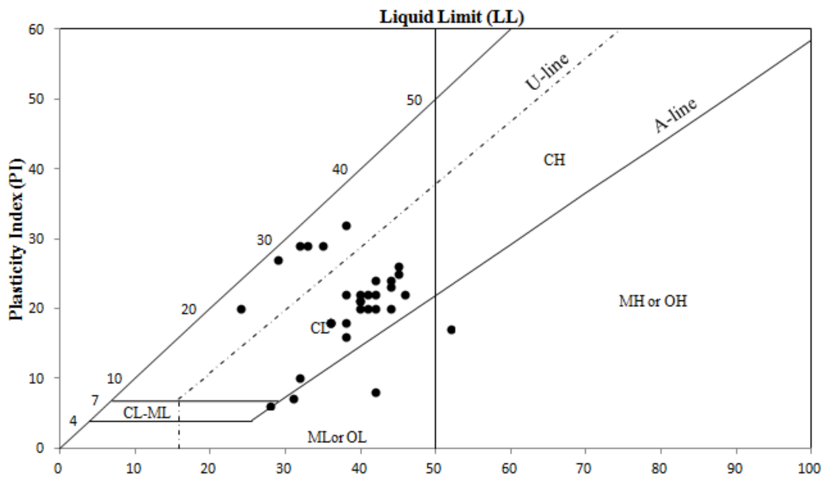

Fig. 5 Position of the samples on a plasticity chart

Table 3 Statistical assessment of the soil samples

Soil properties	Sample amount	Value			
		Min.	Max.	Mean	Std. Deviation
Unit weigth (kN/m^3)	65	18	20.15	18.70	0.384
Water Content (%)	65	4.1	27	16.62	6.5
Consistency limits					
Liquid limit (%)	33	24	52	38. 6	6.13
Plastic limit (%)	33	6	32	20.53	6.41
Plasticity index (%)	33	2	35	18.13	8.13
Grain size distribution					
#4 (%)	65	0.8	57.71	9.93	11.24
#200 (%)	65	7.9	77.47	41.71	16.64

of plastic limit changed between 6% and 32% and average is 20.46%. Average value of plasticity index is determined as 18.5%.The statistical assessment of the soil samples is shown in Table 3.

5. Methodology

In this study, SPT- based method suggested by Seed and Idriss (1971) and Iwasaki *et al*. (1981) has been performed. Scenario earthquakes were produced and, liquefaction analysis was performed. Peak ground surface acceleration ($a_{\max}$) is an important data for scenario earthquakes. Equations of liquefaction analysis are affected by this value. Joyner and Boor (1981), Fukushima *et al*. (1988), Inan *et al*. (1996), Aydan *et al*. (1996), have made various studies upon this value. In this study, Aydan *et al*. (1996) formulated following expression to calculate the horizontal ground acceleration ($a_{\max}$)

$$a_{\max} = 2.8\left(e^{0.9M} * e^{-0.025R} - 1\right) \tag{1}$$

where, M is magnitude, R is the distance from the focus of an earthquake.

5.1 Determination of cyclic stress ratio

Cyclic stress ratio (CSR) characterizes the seismic demand induced by a given earthquake, and it can be determined from peak ground surface acceleration that depends upon site-specific motions (Dixit *et al*. 2012). Seed and Idriss (1971) formulated following expression to calculate the cyclic stress ratio (CSR)

$$CSR = 0.65 \frac{a_{\max}}{g} \frac{\sigma_v}{\sigma'_v} r_d \tag{2}$$

0.65 is a weighing factor to calculate the equivalent uniform stress cycles required generating same pore water pressure during an earthquake; $a_{\max}$ is the peak horizontal ground acceleration; g is acceleration of gravity; σ_v and σ'_v are total vertical overburden stress and effective vertical overburden stress, rd is depth-dependent stress reduction factor (Dixit *et al*. 2012). Youd *et al*. (2001) formulated following expression to calculate the stress reduction factor (r_d)

$$r_d = \frac{1.0 - 0.4113x^{0.5} + 0.04052x + 0.001753x^{1.5}}{1.0 - 0.4177z^{0.5} + 0.05729z - 0.006205z^{1.5} + 0.00121z^2} \tag{3}$$

Iwasaki *et al*. (1981)formulated following expression to calculate the cyclic stress ratio (CSR)

$$CSR = \frac{a_{\max}}{g} \frac{\sigma_{vo}}{\sigma'_{vo}} r_d \tag{4}$$

where, $a_{\max}$ is the peak horizontal ground acceleration; g is the acceleration of gravity; σ_v is the are total vertical overburden stress, σ'_v is the effective vertical overburden stress, r_d is the depth-dependent stress reduction factor.

Depth-dependent stress reduction factor (r_d) calculated from Eq. (5).

$$r_d = 10.0015z \tag{5}$$

where, z is the depth.

5.2 Determination of cyclic resistance ratio

The cyclic resistance ratio (CRR) is defined as the ability of the soil to resist the shear stresses induced by the earthquake. Seed and Idriss (1971) formulated following expression to calculate the cyclic resistance ratio (CRR)

$$CRR = \frac{1}{34-(N_1)_{60}} + \frac{(N_1)_{60}}{135} + \frac{50}{[10(N_1)_{60}+45]^2} - \frac{1}{100} \tag{6}$$

The first step in assessment of liquefaction potential analyses is to compute the corrected blow count $(N_1)_{60}$ values from Eq. (7).

$$(N_1)_{60} = NC_N C_R C_S C_B C_E \tag{7}$$

In Eq. (7), N is measured field SPT blow-count. C_N, C_R, C_S, C_B and C_E are correction factors for effective overburden stress, drilling rod length, type of sampler (with or without liners), bore hole diameter and hammer energy ratio, respectively.

C_N values can be calculated from Eq. (8).

$$C_N = \sqrt{\frac{P_a}{\sigma'_v} \leq 1.7} \tag{8}$$

In this equation, σ'_v is the vertical effective stress and P_a is atmosphere pressure (100 kPa).

The C_R values are recommended are shown in Table 4 (Youd *et al*. 2001).

C_S is for SPT samplers used without a sample liner. C_S value is 1.0 for a standard sampler without liner. Otherwise, C_S value is 1.2 for samplers with liner. C_B correction factor values are recommended by Robertson and Fear (1996). These values are shown in Table 5.

Table 4 Rod length correction with respect the depth

Depth (d)	Correctionfor road length, (C_R)
d < 3 m	0.75
d = 3-4 m	0.80
d = 4-6 m	0.85
d = 6-10 m	0.95
d = 10-30 m	1.0

Table 5 Correction factor for borehole diameter

Diameter of borehole	C_B
65 to 115 mm	1.00
150 mm	1.05
200 mm	1.15

Table 6 Correction factor for hammer energy ratio

Country	Hammer type	Hammer release	C_E
United States	Safety	Rope and pulley	1.0
United States	Donut	Rope and pulley	0.75
Japan	Donut	Rope and pulley, special throw release	1.1
Japan	Donut	Free rall	1.1

Table 7 Unit weight and average grain diameter values

Unit weight γ_n (kN /m^3)	Average grain diameter D_{50} (mm)
17	0.02
17.5	0.025
18	0.04
18.5	0.10
19.5	0.15
20	0.35
20	0.6
21	2.0

The correction factor and energy ratio values are recommended by Seed *et al*. (1985). C_E values are shown in Table 6.

Iwasaki *et al*. (1981) formulated following expression to calculate the cyclic resistance ratio (CRR):

For 0.04 mm $\leq D_{50} \leq$ 0.6 mm

$$CRR = 0.0882\sqrt{\frac{N}{\sigma'_{vo} + 0.7}} + 0.225\log\frac{0.35}{D_{50}} \tag{9a}$$

For 0.6 mm $\leq D_{50} \leq$ 1.5 mm

$$CRR = 0.0882\sqrt{\frac{N}{\sigma'_{vo} + 0.7}} - 0.05 \tag{9b}$$

where, D_{50} is average grain diameter and these values are shown in Table 7, N is the field SPT blow counts, σ'_v is the effective vertical overburden stress, r_d is the depth-dependent stress reduction factor.

5.3 Determination of factor of safety

The potential for liquefaction is described in terms of a factor of safety against liquefaction (Kramer *et al*. 2007). The factor of safety against liquefaction (F_S) determined by

$$F_S = \frac{CRR}{CSR} MSF \tag{10}$$

Table 8 Liquefaction potential categories

Liquefaction potential (F_S)	Liquefaction potential
≤ 0	Liquefiable
$0 < F_S \leq 1.2$	Marginally liquefiable
$1.2 < F_S$	Non-liquefiable

Table 9 Liquefaction potential categories suggested by Iwasaki et al. (1982)

Liquefaction potential index (I_P)	Liquefaction potential
0	Non-liquefiable
$0 < I_P \leq 5$	Low
$5 < I_P \leq 15$	High
$15 < I_P$	Very high

$$MSF = 10^{2.24} / M^{2.56} \tag{11}$$

where *MSF* is the magnitude scaling factor, *M* is the moment magnitude of earthquake.

The factor of safety values are classified three categories, namely, liquefiable, marginally liquefiable and, non-liquefiable (Table 8).

5.4 Determination of liquefaction potential index

The severity of foundation damage caused by liquefaction depends to a great extent on the severity of liquefaction, which cannot be evaluated solely by the factor of safety (F_S) against liquefaction (Ulusay and Kuru 2003). In order to quantify the severity of liquefaction, Iwasaki *et al*. (1982) suggested the liquefaction potential index, I_P, defined as follows.

$$I_P = \int_0^{20} F(z) W(z) dz \tag{12}$$

where, *z* is depth from the ground surface in meters.

$$F(z) = 0 \quad \text{for} \quad F_S \geq 1.0 \tag{13a}$$

$$F(z) = 1 - F_S \quad \text{for} \quad F_S < 1.0 \tag{13b}$$

$$W(z) = 10 - 0.5z \quad \text{for} \quad z < 20\,\text{m} \tag{14a}$$

$$W(z) = 0 \quad \text{for} \quad z > 20\,\text{m} \tag{14b}$$

The following equation is used in cases where more than one layer of soils

$$I_P = \sum_i^n F(z) W(z) H \tag{15}$$

where *z* is depth of layer midpoint in meters, *n* is number of soil layer in meters, *H* is layer thickness in meters. $W(z)$ calculates using Eqs. (14a) and (14b).

As a result of evaluations, Iwasaki *et al*. (1982) proposed classification categories called as non-liquefiable, low, high, and very high for liquefaction potential (Table 9).

6. Assessment of liquefaction potential

The assessment of the liquefaction potential is one of the critical issues in geotechnical earthquake engineering. In this study, liquefaction potential has been determined with the SPT-based method by using records of 50 boreholes from the standard penetration tests in the study area. It was determined by Seed and Idriss (1971) and Iwasaki *et al*. (1981) methods using SPT values in Erzincan city center. The liquefaction assessments are carried out MATLAB programs were written using these methods. Calculations were carried out with this program. First, scenario earthquakes were produced. Magnitudes of earthquake have been selected as M = 6, M = 6.5, and M = 7.0. Peak ground surface acceleration (a_{max}) for these magnitudes of earthquakes was determined using Eq. (1) suggested by Aydan *et al*. (1996). In the 1992 Earthquake, distance from the focus of earthquake (R) was measured as 7.7 km from the city center (Saatcıoglu and Bruneau 1993). In this study, the calculations were made using this value. The calculated a_{max} (peak ground surface acceleration) and *MSF* (magnitude scaling factor) values are shown in Table 10.

Then, the corrected values from the measured SPT blow counts ($(N_1)_{60}$) were calculated using Eq. (7). C_S, C_B, C_R and C_E values for the study area were selected 1.0, 1.0, 1.05, 1.0 respectively. Finally, the cyclic stress ratio (*CSR*) and the cyclic resistance ratio (*CRR*) were calculated. F_S (factor of safety) values for the study area were determined using Eq. (10) according to Seed and Idriss (1971) and Iwasaki *et al*. (1981) methods. The results of the analysis are presented with Table 11. Table 11 was prepared using lowest N values. As a result of these analyses, some regions: namely, private hospital, hospital (1), state building (3) consists of clayey soils. According to Seed and Idriss method, in these areas, $(N_1)_{60}$ values calculated greater than 30. So, in these areas, soil liquefaction was not observed for magnitudes (6.0, 6.5, 7.0).

Liquefaction potential index was defined by the I_p (liquefaction potential index) based on the method of Iwasaki *et al*. (1982). The liquefaction potential index is useful for spatial analysis of liquefaction potential because it allows the two-dimensional representation of a three-dimensional phenomenon (i.e., F_S vs. depth), which is ideal for liquefaction potential maps (Luna and Frost 1998). Four classes were determined based on the I_p values. The boundaries of these classes were determined at 0 for the non-liquefaction class, 0 to 5 for the low liquefaction class, 5 to 15 for the high liquefaction class, and greater than 15 for the very high liquefaction class (Table 9). The I_P (liquefaction potential index) values are calculated '0' for magnitude of 6.0 in the all study area. The I_P values are presented with tables for magnitudes of 6.5 and 7.0 (Tables 12-13). Also, pie

Table 10 Peak ground surface acceleration (a_{max}) and magnitude scaling factor (MSF) values for different magnitudes of earthquakes

Magnitude (M)	Peak ground surface acceleration (a_{max})	Magnitude scaling factor (MSF)
6.0	0.52g	1.77
6.5	0.82g	1.44
7.0	1.27g	1.19

Table 11 Computation of F_S for earthquake magnitudes (M = 6.0, M = 6.5 and M = 7.0)

Location	Depth (m)	M = 6.0		M = 6.5		M = 7.0	
		F_S (Seed and Idriss 1971)	F_S (Iwasaki *et al.* 1981)	F_S (Seed and Idriss 1971)	F_S (Iwasaki *et al.* 1981)	F_S (Seed and Idriss 1971)	F_S (Iwasaki *et al.* 1981)
State building (1)	4	2.37	1.79	1.22	0.93	0.64	0.49
	8	1.55	1.66	0.78	0.86	0.41	0.45
	12	1.35	1.78	0.69	0.92	0.37	0.48
	16	1.33	1.66	0.68	0.86	0.36	0.45
	20	1.26	1.69	0.65	0.87	0.34	0.46
Private hospital	12	1.33	1.60	0.69	0.83	0.36	0.43
	15	1.37	1.61	0.72	0.84	0.37	0.44
	18	1.42	1.64	0.74	0.85	0.39	0.45
Hospital (2)	3	$(N_1)_{60}$ >30	1.78	$(N_1)_{60}$ >30	0.92	$(N_1)_{60}$ >30	0.48
	7.5	1.64	1.61	0.85	0.83	0.44	0.44
State building (2)	3	1.16	0.85	0.60	0.44	0.31	0.23
	6	1.42	1.47	0.73	0.76	0.38	0.41
	9	1.28	0.92	0.66	0.47	0.35	0.25
Home for the aged	3	$(N_1)_{60}$ > 30	1.89	$(N_1)_{60}$ > 30	0.97	$(N_1)_{60}$ > 30	0.51
	6	$(N_1)_{60}$ > 30	2.02	$(N_1)_{60}$ > 30	1.04	$(N_1)_{60}$ > 30	0.55
	9	$(N_1)_{60}$ > 30	1.83	$(N_1)_{60}$ > 30	0.95	$(N_1)_{60}$ > 30	0.53
	12	1.48	1.68	0.76	0.87	0.40	0.49
Treatment plant	3	$(N_1)_{60}$ > 30	1.14	$(N_1)_{60}$ > 30	0.59	$(N_1)_{60}$ > 30	0.31
	6	1.32	1.09	0.68	0.51	0.36	0.27
	9	$(N_1)_{60}$ > 30	0.98	$(N_1)_{60}$ > 30	0.50	$(N_1)_{60}$ > 30	0.36
Industry area	3	$(N_1)_{60}$ > 30	1.89	$(N_1)_{60}$ > 30	0.97	$(N_1)_{60}$ > 30	0.51
	6	$(N_1)_{60}$ > 30	2.02	$(N_1)_{60}$ > 30	1.04	$(N_1)_{60}$ > 30	0.55
	9	$(N_1)_{60}$ > 30	1.83	$(N_1)_{60}$ > 30	0.95	$(N_1)_{60}$ > 30	0.53
	12	1.48	1.68	0.76	0.87	0.40	0.49

charts showing the areas of the liquefaction potential index were prepared (Fig. 6). According to liquefaction potential index values, for the M = 6.0, all study area having the category of non-liquefiable for Seed and Idriss (1971) and Iwasaki *et al*. (1981) For the M = 6.5, low liquefied areas are 23.17% and 29.26% for Seed and Idriss (1971) and Iwasaki *et al*. (1981), respectively. The high liquefied areas are 15.85% and 31.71%, respectively. The very high liquefied areas are 7.13% and 20.74%, respectively. For the M = 7.0, the low liquefied areas were not observed. The high liquefied areas are 8.54% and 14.63% for Seed and Idriss (1971) and Iwasaki *et al*. (1981), respectively. The very high liquefied areas are 43.92% and 69.52%, for Seed and Idriss (1971) and Iwasaki *et al*. (1981), respectively.

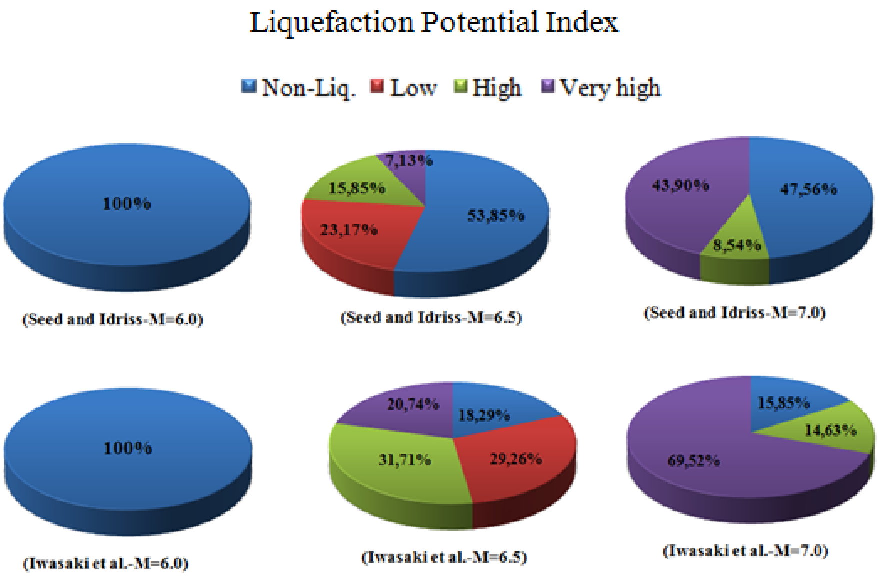

Fig. 6 Pie charts showing the areas of the liquefaction potential index

Table 12 Computation of I_P for earthquake magnitude (M = 6.5)

Borehole No.	I_P (Seed and Idriss 1971)			I_P (Iwasaki *et al*. 1981)		
	Depth (m)			Depth (m)		
	3	6	9	3	6	9
SK-1	1.8	3.48	9.48	5.04	5.04	7.24
SK-2	0	4.48	11.48	0	0.84	2.84
SK-3	0	1.4	6.2	0	0.28	2.88
SK-4	0	1.68	7.68	1.44	1.72	4.92
SK-5	0	6.16	12.18	2.52	6.44	8.36
SK-19	0	4.65	4.65	2.22	5.98	5.98
SK-20	0	4.97	4.97	2.77	6.75	6.75
SK-21	0	3.32	3.32	2.77	7.74	7.74
SK-22	0	3.32	3.32	3.05	8.02	8.02
SK-23	0	4.97	4.97	3.05	6.81	6.81
SK-24	0	3.32	3.32	2.77	7.74	7.74
SK-25	0	4.65	4.65	2.22	7.19	7.19
SK-26	0	0	0	4.44	8.09	8.09
SK-27	10.27	10.27	11.77	15.54	21.12	31.06
SK-28	11.38	15.8	21.8	15.54	20.42	30.17

Table 12 Continued

Borehole No.	I_P (Seed and Idriss 1971)			I_P (Iwasaki *et al*. 1981)		
	Depth (m)			Depth (m)		
	3	6	9	3	6	9
SK-29	11.38	15.8	21.8	15.54	20.42	30.17
SK-30	0	0	0	0.83	2.69	2.69
SK-31	0	0	0	1.38	1.38	1.38
SK-32	0	0	0	0.83	2.69	2.69
SK-33	0	7.44	15.5	11.37	22.76	32.51
SK-34	0	0	0	10.82	21.78	30.75
SK-35	0	0	0	10.82	22.21	31.96
SK-36	0	7.44	15.5	11.37	22.76	32.51
SK-43	0	0	0	0.83	2.69	2.69
SK-44	0	0	0	1.38	1.38	1.38
SK-45	0	0	0	0.83	2.69	2.69
SK-46	0	0	0	0.83	2.69	2.69
SK-47	0	0	0	1.38	1.38	1.38
SK-48	0	0	0	0.83	2.69	2.69
SK-49	0	0	0	0.83	2.69	2.69
SK-50	0	0	0	1.38	1.38	1.38

Table 13 Computation of I_P for earthquake magnitude (M = 7.0)

Borehole No	I_P (Seed and Idriss 1971)			I_P (Iwasaki *et al*. 1981)		
	Depth (m)			Depth (m)		
	3	6	9	3	6	9
SK-1	18	32.28	44.8	19.8	32.68	43.28
SK-2	15.12	30.8	44	18	31.72	42.72
SK-3	0	14	26	12.4	27.28	37.48
SK-4	12.6	26.88	39.48	16.2	30.48	41.08
SK-5	12.96	29.48	42.08	16.2	30.48	41.08
SK-19	0	17.92	17.92	14.43	33.02	33.02
SK-20	0	15.26	15.26	14.43	32.35	32.35
SK-21	0	17.25	17.25	14.43	32.68	32.68
SK-22	0	17.25	17.25	14.71	32.96	32.96
SK-23	0	17.58	17.58	14.71	33.3	33.3
SK-24	0	17.25	17.25	14.43	32.68	32.68
SK-25	0	17.92	17.92	14.43	33.02	33.02
SK-26	0	11.94	11.94	14.15	31.73	31.73
SK-27	17.76	18.44	27.26	21.36	35.08	49.68
SK-28	19.14	19.83	32.02	21.36	35.08	49.68

Table 13 Continued

Borehole No	I_P (Seed and Idriss 1971)			I_P (Iwasaki *et al.* 1981)		
	Depth (m)			Depth (m)		
	3	6	9	3	6	9
SK-29	19.15	32.64	44.83	21.36	35.08	49.68
SK-30	0	0	0	13.59	25.44	34.07
SK-31	0	0	0	13.88	24.34	32.22
SK-32	0	0	0	13.59	25.44	34.07
SK-33	0	14.88	28.01	19.15	36.12	50.56
SK-34	0	0	0	18.59	35.1	48.78
SK-35	0	0	0	18.59	35.55	50
SK-36	0	14.88	28.01	19.15	36.12	50.56
SK-43	0	0	0	13.59	25.44	34.07
SK-44	0	0	0	13.88	24.34	32.22
SK-45	0	0	0	13.59	25.44	34.07
SK-46	0	0	0	13.59	25.44	34.07
SK-47	0	0	0	13.88	24.34	32.22
SK-48	0	0	0	13.59	25.44	34.07
SK-49	0	0	0	13.88	24.34	32.22
SK-50	0	0	0	13.59	25.44	34.07

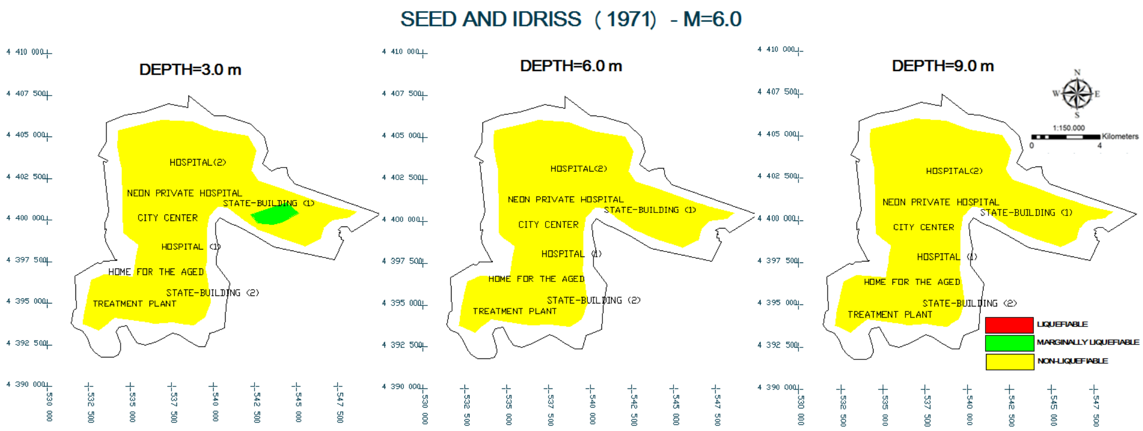

Fig. 7 Liquefaction potential maps according to F_S values (Seed and Idriss (1971)-M = 6.0)

7. Production of liquefaction potential maps

Liquefaction potential maps were produced using ArcGis 10 programme Arcinfo Module Spatial Analysis Arctoolbox IDW (inverse distance weighted technique). IDW is interpolation analysis one of the widely used. The IDW interpolator assumes that each point has a local influence that diminishes with distance and as such weights more the points that are closer to the

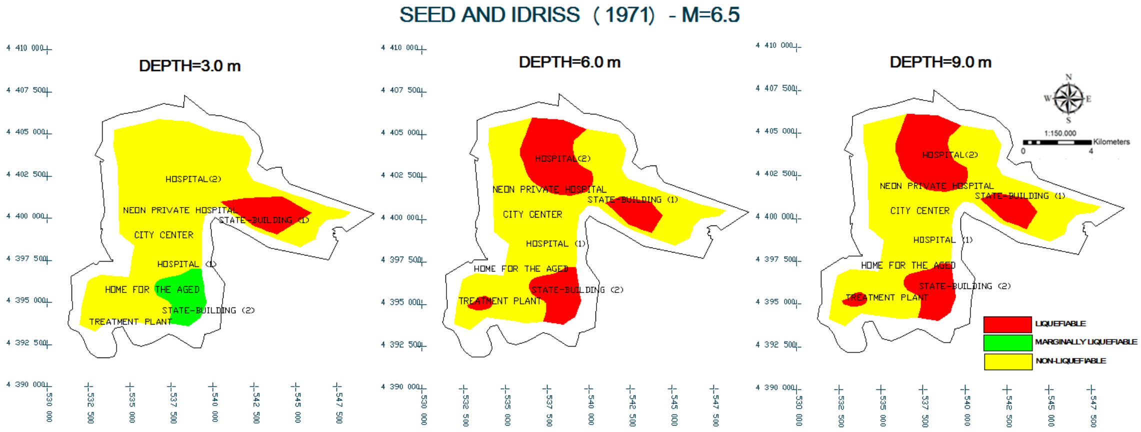

Fig. 8 Liquefaction potential maps according to F_S values (Seed and Idriss (1971)-M = 6.5)

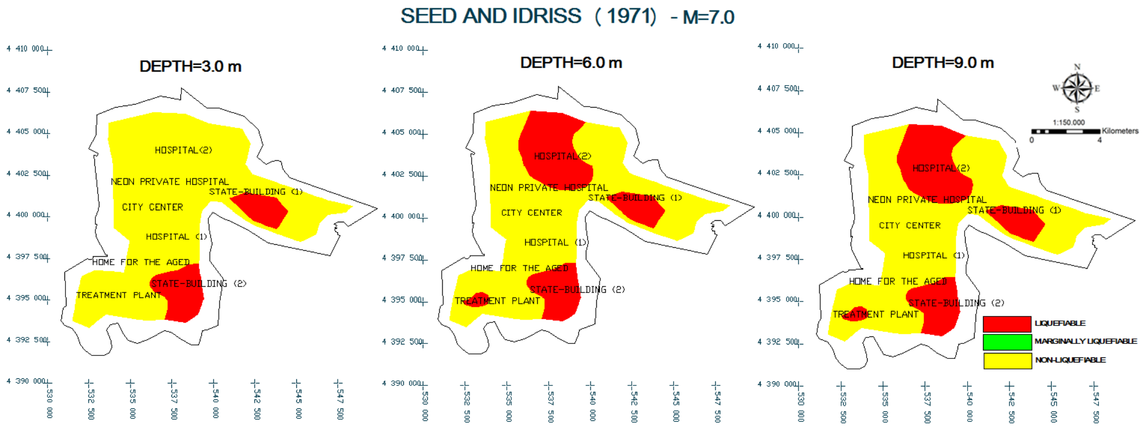

Fig. 9 Liquefaction potential maps according to F_S values (Seed and Idriss (1971)-M = 7.0)

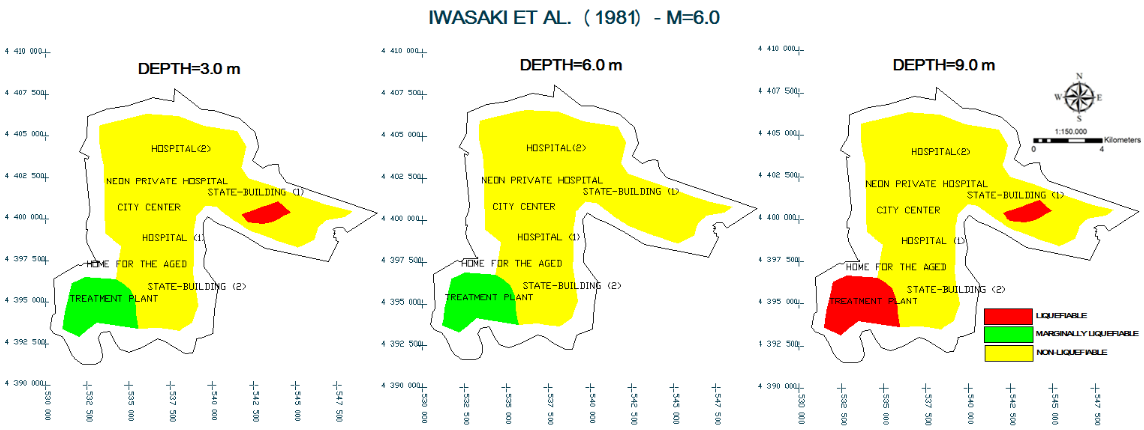

Fig. 10 Liquefaction potential maps according to F_S values (Iwasaki *et al*. (1981)-M = 6.0)

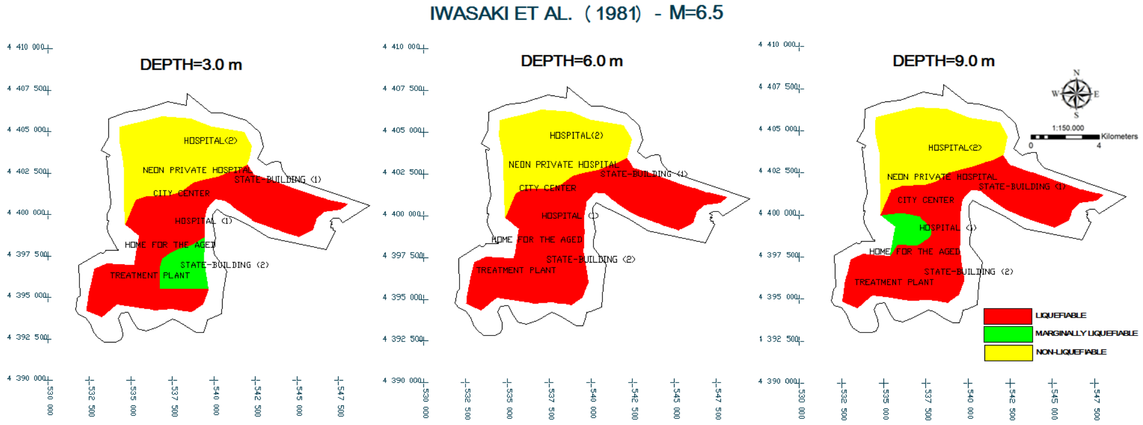

Fig. 11 Liquefaction potential maps according to F_S values (Iwasaki *et al*. (1981)-M = 6.5)

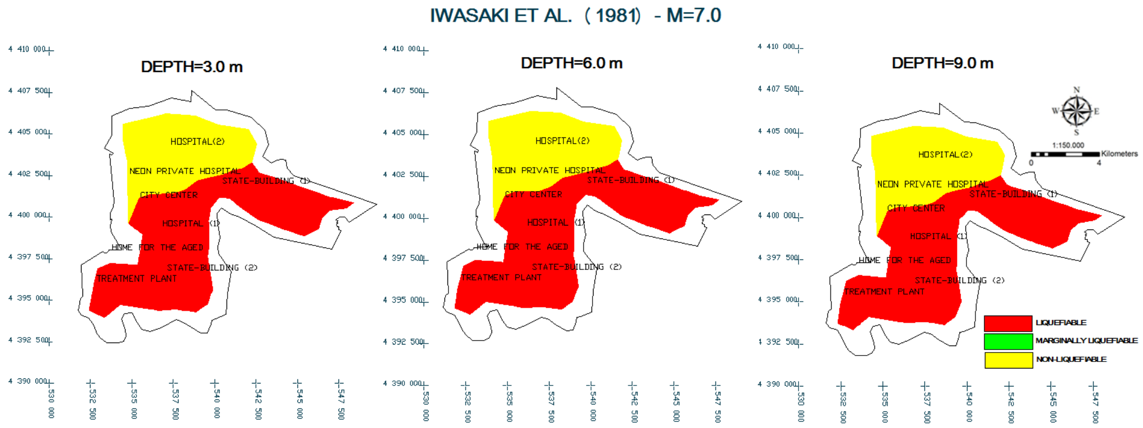

Fig. 12 Liquefaction potential maps according to F_S values (Iwasaki *et al*. (1981)-M = 7.0)

processing cell than those farther away. The spline interpolator fits a surface with minimum curvature through the input points and is ideal for elevation, water surface, and geological contours (Antoniou *et al*. 2008).

Liquefaction potential maps were prepared for different earthquake magnitudes and depth intervals (3-6-9 m) by interpolating most convenient F_S values depending on 50 borehole data of study area. The liquefaction potential is classified into three categories, namely non- liquefiable, marginally liquefiable and liquefiable areas. These maps are shown in Figs. 7-12. The maps produced using three colors, namely nonliquefiable-yellow, marginally liquefiable-green and liquefiable-red.

According to Seed and Idriss (1971) method, when Mis equal to 6.0, liquefiable region was not observed for depths of 6 m and 9 m because results are greater than 1.2. Marginally liquefiable regions were observed around State building (1) for depth of 3 m. When Mis equal to 6.5, liquefiable region were observed around State building (1) for depth of 3 m. Also, marginally liquefiable regions were observed around State building (2) and home for aged. Liquefiable region was observed for depths of 6 m and 9 m at the some regions. When Mis equal to 7.0, liquefiable region was observed for depths of 3 m, 6 m and 9 m because results are less than 1.0.

According to Iwasaki *et al*. (1981) method, when Mis equal to 6.0, liquefiable region was not observed for depths of 3 m, 6 m and 9 m around city center. Marginally liquefiable and liquefiable regions were observed around treatment plant and State building (2). When Mis equal to 6.5, liquefiable regions were observed for depths of 3 m, 6 m and 9 m the south of the city center. Marginally liquefiable regions were observed around State building (2) and hospital (1) for depths 3 m and 9 m. When Mis equal to 7.0, liquefiable region was not observed for depths of 3 m, 6 m and 9 m the north of the city center.

Liquefaction potential index maps were prepared for different earthquake magnitudes and depth intervals (3-6-9 m). The liquefaction potential is classified into four categories, namely non-liquefiable, low, high and very high. These maps are shown in Figs. 13-18. The maps produced using four colors, namely non liquefiable-yellow, low-green, high-pink and very high-red. According to Seed and Idriss (1971) - Iwasaki *et al*. (1981), when Mis equal to 6.0,

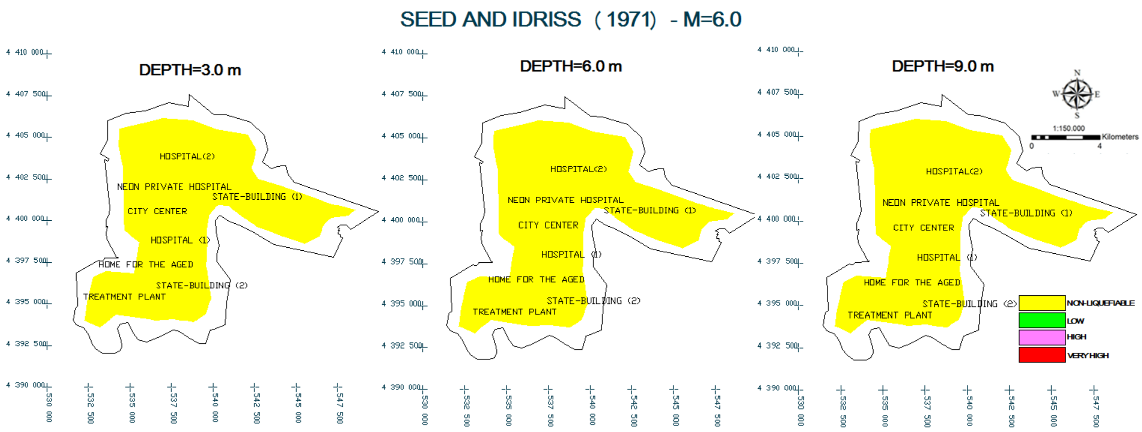

Fig. 13 Liquefaction potential index maps (Seed and Idriss (1971)-$M = 6.0$)

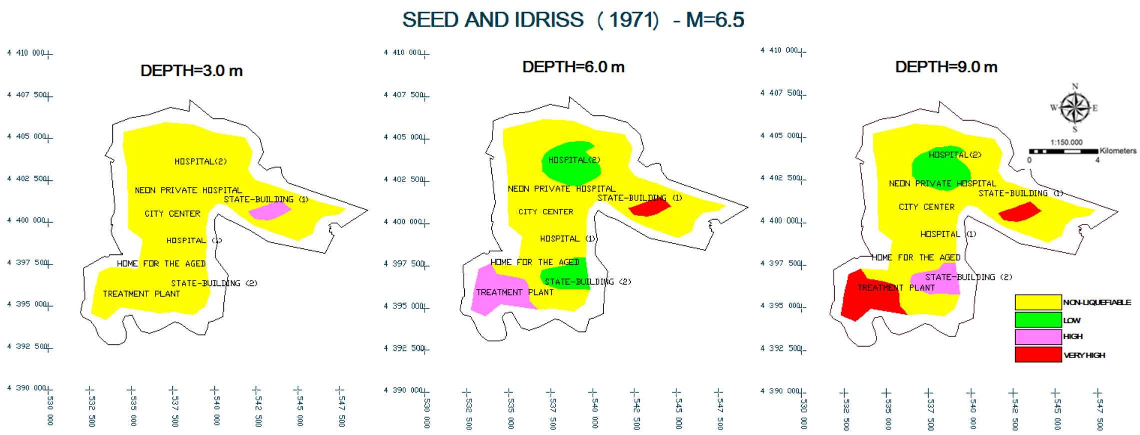

Fig. 14 Liquefaction potential index maps (Seed and Idriss (1971)-$M = 6.5$)

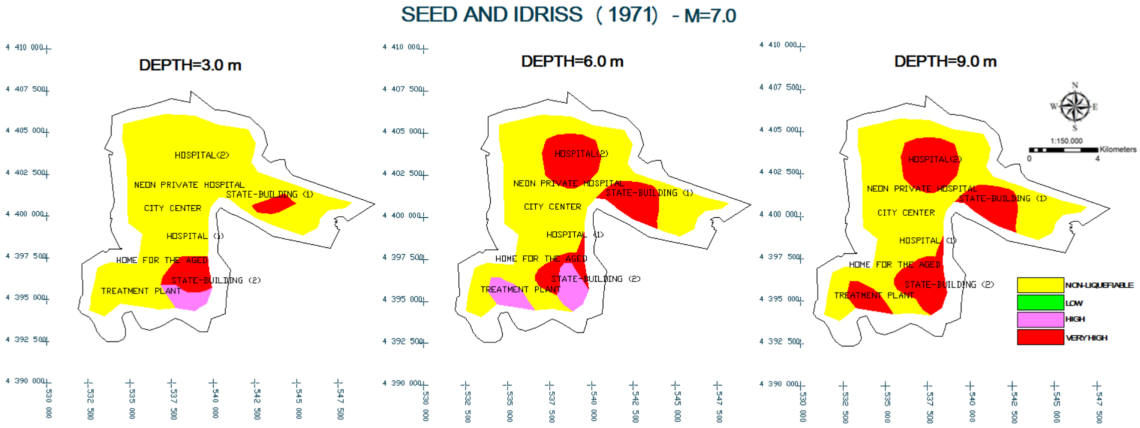

Fig. 15 Liquefaction potential index maps (Seed and Idriss (1971)-$M = 7.0$)

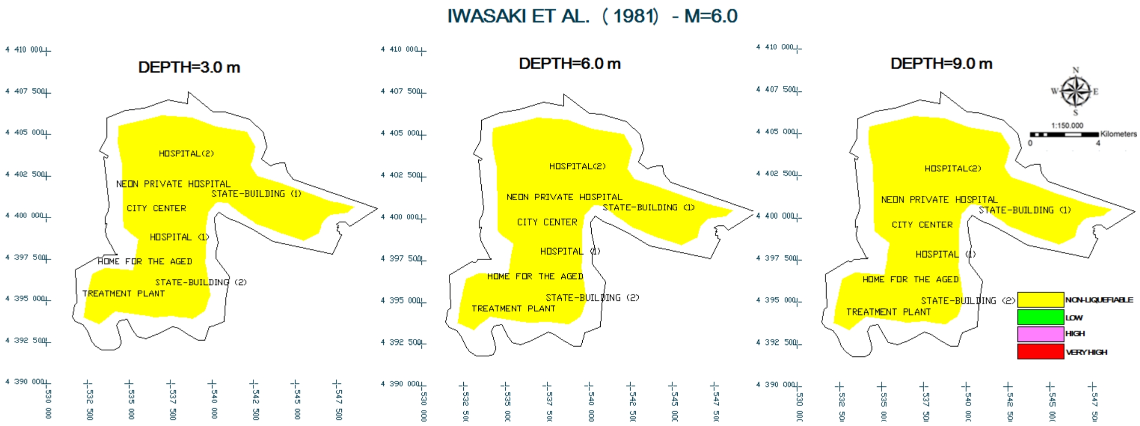

Fig. 16 Liquefaction potential index maps (Iwasaki *et al.* (1981)-$M = 6.0$)

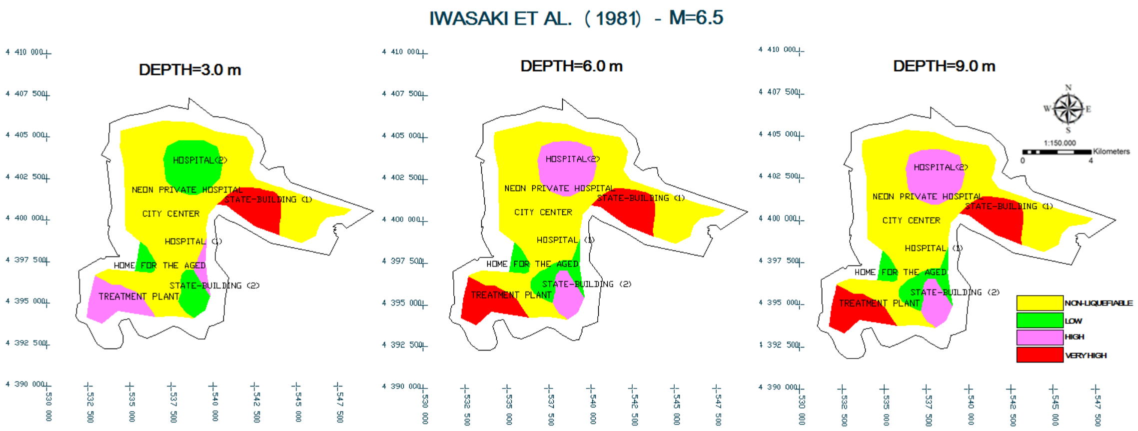

Fig. 17 Liquefaction potential index maps (Iwasaki *et al.* (1981)-$M = 6.5$)

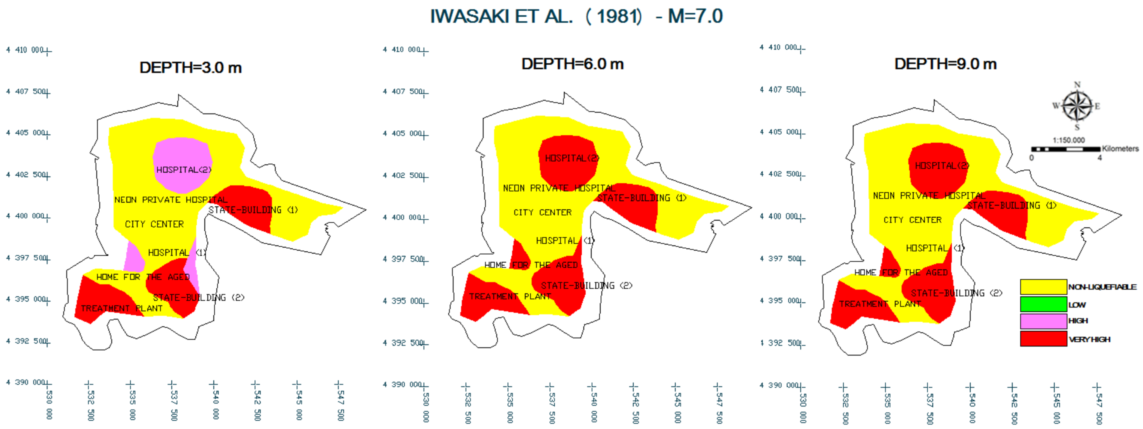

Fig. 18 Liquefaction potential index maps (Iwasaki *et al.* (1981)-$M = 7.0$)

liquefiable regions were not observed for depths of 3 m, 6 m and 9 m. When Mis equal to 6.5, very high liquefiable regions were observed around treatment plant and state building (2). When Mis equal to 7.0, very high liquefiable regions were observed the north and south of the city center.

7. Conclusions

Erzincan Basin, where soil conditions are highly heterogeneous, is composed of alluvial deposits of sand and gravel with very small amounts of clay and silt. Due to the Euphrates River near the city of Erzincan, underground water level is quite high. Assessment of the liquefaction potential is one of the critical issues in Erzincan Province due to soil conditions, high level of ground water, and earthquake hazard. In this study, Liquefaction potential for different earthquake magnitudes (6.0, 6.5, 7.0) were determined using SPT data. Liquefaction potential analyses were examined using two methods, namely Seed and Idriss (1971), Iwasaki *et al.* (1981). Furthermore, liquefaction potential index is investigated by Iwasaki *et al.* (1982). Liquefaction potential maps and liquefaction potential index maps of the area by using ArcGIS 10.0 Software and IDW interpolation method were prepared for different earthquake magnitudes and different depths.

- According to Seed and Idriss (1971) methods, F_S values were calculated greater than 1.2 for all study area for 6.0 magnitude earthquake. Liquefaction potential of less than 1 were mainly located in the south, north, and east sections of the city center for 6.5 and 7.0 magnitude earthquakes.
- According to Iwasaki *et al.* (1981) methods, liquefaction potential of less than 1 were mainly located in the south sections of the city center for 6, 6.5 and 7.0 magnitude earthquakes.
- From the result of the liquefaction analyses, while liquefiable regions were not observed according to Seed and Idriss (1971) methods, 10% of study area was liquefiable according to Iwasaki *et al.* (1981) methods for $M = 6$. While less than 50% of study area was liquefiable according to Seed and Idriss (1971) methods, more than 50% of study area was liquefiable according to Iwasaki *et al.* (1981) methods for $M = 6.5$ and $M = 7$.

- According to Seed and Idriss (1971) and Iwasaki *et al*. (1981) methods, I_p values were calculated 0 for all study area for 6.0 magnitude earthquake. That is, all study area was categorized as non-liquefiable.
- Liquefaction potential index of greater than 15 (very high liquefiable) and between 5 and 15 (high liquefiable) were mainly located in small regions of the south, north, and east sections of the city center for 6.5 and 7.0 magnitude earthquakes. I_p values were calculated between 0 and 5 (low liquefiable) in the south and north sections of the city center for 6.5 magnitude earthquakes. Low liquefiable areas were not observed in the city center for 7.0 magnitude earthquakes. It can be observed from the liquefaction potential index maps that severe damages is likely to occur at many sites in the city during intense seismic activity. These maps can also be used effectively for seismic safety plans and in the seismic hazard mitigation programs.
- In general, the results showed that liquefaction potential changes with earthquake magnitudes. Result of analyses indicates that presence of ground water and sandy-silty soils increases the liquefaction potential with the seismic features of the region. The authors of this work believe that the liquefaction potential and liquefaction potential index maps can be used to prevent loss of life and to mitigate property losses in Erzincan Province. Soil investigation should be done carefully in the construction sites which have high liquefaction potential and necessary measures should be taken.

References

Ansal, A. and Tönük, G. (2007), "Source and site factors in microzonation", *Earthq*. *Geotech*. *Eng*., **6**, 73-92.

Antoniou, A.A., Papadimitriou, A.G. and Tsiambaos, G. (2008), "A geographical information system managing geotechnical data for Athens (Greece) and its use for automated seismic microzonation", *Nat. Hazard*., **47**(3), 369-395.

Aydan, Ö., Sezaki, M. and Yarar, R. (1996), "The seismic characteristic of Turkish earthquakes", *Proceedings of the 11th World Conference on Earthquake Engineering*, Mexico, pp. 1-8.

Choobbasti, A.J., Saadati, M. and Tavakoli, H.R. (2012a), "Seismic response of pile foundations in liquefiable soil: Parametric study", *Arab. J. Geosci*., **5**(6), 1307-1315.

Choobbasti, A.J., Vahdatirad, M.J., Torabi, M., Firouzian, S. and Barari, A. (2012b), "Assessmentof soil liquefaction potential based on numerical method- a case study of an urban railway project", *Arab*. *J*. *Geosci*., **5**(4), 545-554.

Choobbasti, A.J., Ghalandarzadeh, A. and Esmaeili, M. (2013), "Experimental study of the grading characteristic effect on the liquefaction resistance of various graded sands and gravelly sands", *Arab*. *J*. *Geosci*., **7**(7), 2739-2748.

Dixit, J., Dewaikar, D.M. and Jangid, R.S. (2012), "Assessment of liquefaction potential index for Mumbai city", *Nat*. *Hazard*. *Earth Syst*. *Sci*., **12**, 2759-2768.

Emre, O., Kondo, H., Ozalp, S., Elmaci, H. and Kurcer, A. (2010), "Fault geometry and slip distribution associated with the 1939 Erzincan Earthquake (M: 7.9), North Anatolian Fault", *EGU General Assembly 2010*, Vienna, Austria, May.

Fukushima, Y., Tamaka, T. and Kataoka, S. (1998), "A new attenuation relationship for peak ground accelerations derived from strong motion accelograms", *Proceedings of the 9th WCEE*, Tokyo, Japan, August.

Gurenko, E., Lester, R., Mahul, O. and Gonulal, S.O. (2006), "Earthquake insurance in Turkey, history of the Turkish catastrophe insurance pool", *The International Bank for Reconstruction and Development / The World Bank*, 136 p.

Inan, E., Colakoglu, Z., Koc, N., Bayulke, N. and Coruh, E. (1996), "Catalogue of earthquakes between 1976-1996 with acceleration records", ERD, General Directorate of Disaster Affairs of Public Works and Settlement Ankara, p. 150.
Iwasaki, T., Tokida, K. and Tatsuoka, F. (1981), "Soil liquefaction potential evaluation with use of the simplified procedure", *International Conference on Recent Advances in Geotechnical Earthquake Engineering and Soil Dynamics*, St. Louis, MO, USA, April-May, pp. 209-214.
Iwasaki, T., Tokida, K., Tatsuoka, F., Watanabe, S., Yasuda, S. and Sato, H. (1982), "Microzonation for soil liquefaction potential using simplified methods", *Proceedings of the 3rd International Conference on Microzonation*, Seattle, WA, USA, June-July, **3**, 1319-1330.
Joyner, W.B. and Boore, D.M. (1981), "Peak horizontal acceleration and velocity from strong motion records including records from the 1979 imperial valley, California Earthquake", *Bull. Seis. Soc. Am.*, **71**(6), 2011-2038.
Kaypak, B. (2002), "Determination of 3-D velocity structure of the Erzincan basin by local earthquake tomography", Ph.D. Thesis, Istanbul University, Graduate School of Natural and Applied Sciences, 224 p.
Kramer, S.L. and Mayfield, R.T. (2007), "Return period of soil liquefaction", *J. Geotech. Geoenviron. Eng.*, **133**(7), 802-813.
Krim, A., Zitouni, Z.A., Arab, A. and Mostéfa, B. (2013), "Identification of the behavior of sandy soil to static liquefaction and microtomography", *Arab. J. Geosci.*, **6**(7), 2211-2224.
Luna, R. and Frost, J.D. (1998), "Spatial liquefaction analysis system", *J. Comput. Civil Eng.*, **12**(1), 48-56.
Mhaske, S.Y. and Choudhury, D. (2010), "GIS-based soil liquefaction susceptibility map of Mumbai city for earthquake events", *J. Appl. Geophys.*, **70**(3), 216-225.
Orhan, A., Turkoz, M. and Tosun, H. (2013), "Preliminary hazard assessment and site characterization of Meselik campus area, Eskisehir-Turkey", *Nat. Hazard. Earth Syst. Sci.*, **13**, 75-84.
Robertson, P.K. and Fear, C.E. (1995), "Liquefaction of sands and its evaluation" Proceedings *of the 1st International Conference on Earthquake Geotechnical Engineering*, Tokyo, Japan, June, Preprint Volume, pp. 91-128.
Robertson, P.K. and Wride, C.E. (1998), "Evaluating cyclic liquefaction potential using the cone penetration test", *Can. Geotech. J.*, **35**(3), 442-459.
Saatcioglu, M. and Bruneau, M. (1993), "Performance of structures during the 1992 Erzincan earthquake", *Can. J. Civ. Eng.*, **20**(2), 305-325.
Samui, P. and Sitharam, T.G. (2011), "Machine learning modeling for predicting soil liquefaction susceptibility", *Nat. Hazards Earth Syst. Sci.*, **11**, 1-9.
Sandoval, E.A. and Pando, M.A. (2012), "Experimental assessment of the liquefaction resistance of calcareous biogenous sands", *Earth Sci. Res. J.* **16**(1), 55-63.
Seed, H.B. and Idriss, I.M. (1971), "Simplified procedure for evaluating soil liquefaction potential", *J. Soil Mech. Found. Div.*, *ASCE*, **97**(9), 1249-1273.
Seed, H.B., Tokimatsu, K., Harder, L.F. and Chung, R. (1985), "Influence of SPT procedures in soil liquefaction resistance evaluations", *J. Geotech. Eng.*, *ASCE*, **111**(12), 1425-1445.
Seed, H.B. and De Alba, P. (1986), "Use of SPT and CPT tests for evaluating the liquefaction resistance of soils", *Proceedings of the ASCE Specialty Conference In-Situ'86*: Use *of In-Situ Tests in Geotechnical Engineering*, Blacksburg, VA, USA, pp. 281-302.
Seed, R.B., Cetin, K.O., Bray, J.D., Faris, A., Kammerer, A.M., Kayen, R.E., Moss, R.E.S., Pestana, J. M., Riemer, M.F., Sancio, R.B. and Wu, J. (2003), "Recent advances in soil liquefaction engineering: A Unified and Consistent Framework", *Proceedings of the 26th Annual ASCE Los Angeles Geotechnical Spring Seminar*, (Keynote Presentation: H.M.S. Queen Mary), Long Beach, CA, USA.
Shooshpasha, I. and Bagheri, M. (2014), "The effects of surcharge on liquefaction resistance of silty sand", *Arab. J. Geosci.*, **7**(3), 1029-1035.
Sonmez, H. and Gokceoglu, C. (2005), "A liquefaction severity index suggested for engineering practice", *Environ. Geology.*, **48**(1), 81-91.
Suzuki, Y., Koyamada, K. and Tokimatsu, K. (1997), "Prediction of liquefaction resistance based on CPT tip resistance and sleeve friction", *Procedings XIV International Conference of Soil Mechanics and*

Foundation Engineering, Hamburg, Germany, pp. 603-606.

Tokimatsu, K. and Yoshimi, Y. (1983), "Empirical correlation of soil liquefaction based on SPT N-value and fines content", *Soil Found*., **23**(4), 56-74.

Tosun, H., Seyrek, E., Orhan, A., Savas, H. and Turkoz, M. (2011), "Soil liquefaction potential in Eskişehir, NW Turkey", *Nat. Hazard. Earth Syst. Sci*., **11**, 1071-1082.

Ulusay, R and Kuru, T. (2004), "1998 Adana-Ceyhan (Turkey) earthquake and preliminary microzonation based on liquefaction potential for Ceyhan Town", *Nat. Hazard*., **32**(1), 59-88.

Yalcın, A., Gokceoglu, C. and Sonmez, H. (2008), "Liquefaction severity map for Aksaray city center (Central Anatolia, Turkey)", *Nat. Hazard. Earth Syst. Sci*., **8**, 641-649.

Youd, T.L., Idriss, I.M., Andrus, R.D., Arango, I., Castro, G., Christian, J.T., Dobry, R., Finn, W.D., Harder, L.F.Jr., Hynes, M.E., Ishihara, K., Koester, J.P., Liao, S.S.C., Marcuson, W.F.III, Martin, G.R., Mitchell, J.K., Moriwaki, Y., Power, M.S., Robertson, P.K., Seed, R.B. and Stokoe, K.II. (2001), "Liquefaction resistance of soils: Summary report from the 1996 NCEER and 1998 NCEER / NSF workshops on evaluation of liquefaction resistance of soils", *J. Geotech. Geoenviron. Eng*., *ASCE*, **127**(10), 817-833.

Zhang, J.L., Zhang, L.M. and Huang, H.W. (2013), "Evaluation of generalized linear models for soil liquefaction probability prediction", *Environ. Earth Sci*., **68**(7), 1925-1933.

JS